A Potent Oligosaccharyl Transferase Inhibitor That Crosses the Intracellular Endoplasmic Reticulum Membrane†

Paula Denney Eason and Barbara Imperiali*

Division of Chemistry and Chemical Engineering, California Institute of Technology, Pasadena, California 91125

Received November 18, 1998; Revised Manuscript Received January 19, 1999

ABSTRACT: Recent work has resulted in the development of potent inhibitors of *oligosaccharyl transferase* (*OT*), the enzyme that catalyzes the cotranslational glycosylation of asparagine [Hendrickson, T. L., Spencer, J. R., Kato, M., and Imperiali, B. (1996) *J. Am. Chem. Soc. 118*, 7636−7637; Kellenberger, C., Hendrickson, T. L., and Imperiali, B. (1997) *Biochemistry 36*, 12554−12559]. However, no specific *OT* inhibitors that function in the cellular environment have yet been reported. The peptide *cyclo*(hex-Amb-Cys)-Thr-Val-Thr-Nph-NH_2 was previously shown to exhibit nanomolar inhibition (K_i = 37 nM) through slow tight binding kinetics [Hendrickson, T. L., Spencer, J. R., Kato, M., and Imperiali, B. (1996) *J. Am. Chem. Soc. 118*, 7636−7637]. Included herein is the redesign of this prototype inhibitor for achieving both passive and active translocation into model membrane systems representing the endoplasmic reticulum (ER). The strategy for passive transport involved the incorporation of a membrane permeable import function previously shown to carry various peptides across the outer as well as the interior cellular membranes [Rojas, M., Donahue, J. P., Tan, Z., and Lin, Y.-Z. (1998) *Nat. Biotechnol. 16*, 370−375]. Assessment of function in intact ER membranes revealed that the inhibitor targeted toward passive diffusion demonstrated concentration-dependent inhibition of two different glycosylation substrates. Thus, this modified inhibitor achieved potent inhibition of glycosylation after being successfully transported through the ER membrane. In the active translocation approach, the lead *OT* inhibitor and a corresponding substrate were redesigned to include features recognized by the transporter associated with antigen processing (TAP). This protein translocates peptides into the lumen of the ER [Heemels, M.-T., Schumacher, T. N. M., Wonigeit, K., and Ploegh, H. L. (1993) *Science 262*, 2059−2063]. However, although acceptance of the cyclized substrate by the TAP receptor was demonstrated *via* efficient transport and glycosylation, the modified inhibitor was not translocated by TAP machinery, and therefore, active translocation was achieved for the modified substrate only. Both of these ER transport methods afforded redesigned *OT* inhibitors that retained their inhibitor properties *in vitro*, regardless of the extensions to the carboxy-terminus of the root inhibitor. The above family of redesigned inhibitors provides a template for generating a transcellular pathway and represents the first step toward *OT* inhibition in intact cells.

Complex protein modification reactions, such as *N*-linked glycosylation of asparagine, are essential for the function and biological diversity of eukaryotic cells. *N*-linked glycosylation is mediated by the membrane-bound enzyme *oligosaccharyl transferase* (*OT*), found associated with the lumenal face of the endoplasmic reticulum (ER)[1] membrane. The transfer of an oligosaccharide from a lipid-linked tetradecasaccharide donor ($Glc_3Man_9GlcNAc_2$P-P-dolichol) to the carboxamide nitrogen of asparagine in a polypeptide chain is catalyzed by *OT*. This transformation represents the first committed step in the *N*-glycosylation of proteins, and only occurs after this nascent polypeptide has been translocated into the ER (*1*). The modified asparagine always occurs within the consensus sequence Asn-Xaa-Thr/Ser (NXT/S), where Xaa is any amino acid except proline (*2*).

Specific inhibitors of the *OT*-catalyzed cotranslational glycosylation of asparagine may ultimately provide insight into this critical eukaryotic modification process. Currently, the microbial product tunicamycin is the most widely used inhibitor of *N*-linked protein glycosylation. This natural product prevents the synthesis of the lipid-linked saccharide donor by blocking the transfer of *N*-acetylglucosamine

† This work was supported by the National Institutes of Health (GM 39334) and an NIH postdoctoral fellowship (GM18959) that was awarded to P.D.E.

* To whom correspondence should be addressed. Telephone: (626) 395-6101. E-mail: imper@caltech.edu.

[1] Abbreviations: α-MEM, α-modified Eagle's medium; AEBSF, 4-(2-aminoethyl)benzenesulfonyl fluoride; Amb, (*S*)-2,4-diaminobutyric acid; ATP, adenosine 5′-triphosphate; Boc, butyloxycarbonyl; Bz, benzoyl; DIPCDI, diisopropylcarbodiimide; DMF, dimethylformamide; DMSO, dimethyl sulfoxide; dpm, disintegrations per minute; DPPC, dolichol-P-P-GlcNAc-GlcNAc; DTT, dithiothreitol; EDTA, ethylenediaminetetraacetic acid; ER, endoplasmic reticulum; Fmoc, 9-fluorenylmethoxycarbonyl; GDP, guanosine 5′-diphosphate; GlcNAc, *N*-acetylglucosamine; HEPES, *N*-(2-hydroxyethyl)piperazine-*N*′-2-ethanesulfonic acid; MHC, major histocompatibility complex; NLT, Bz-Asn-Leu-Thr-NHMe; NP-40, Nonidet P-40; OT, oligosaccharyl transferase; Pbf, pentanethyldihydrobenzofuran; PBS, phosphate-buffered saline; TAP, transporter associated with antigen processing; *t*Bu, *tert*-butyl; TFA, trifluoroacetic acid; TIPS, triisopropylsilane; Tmob, trimethoxybenzyl; UDP, uridine 5′-diphosphate; UTP, uridine 5′-triphosphate.

10.1021/bi982740e CCC: $18.00
Published on Web 04/08/1999

1-phosphate from UDP-*N*-acetylglucosamine to dolichyl phosphate (*3*). However, because this metabolic step occurs very early in the stepwise assembly of the oligosaccharide donor ($Glc_3Man_9GlcNAc_2P$-P-dolichol), the inhibitory activity of tunicamycin is rather indirect. In addition, the structure of tunicamycin is not readily manipulated synthetically (*4*). Finally, while this antibiotic is active at nanomolar concentrations, it works in a time-dependent manner, requiring several cycles before the lipid-linked donor is depleted and glycosylation is arrested (*5*). Therefore, tunicamycin does not specifically target *OT*, nor are its effects immediate.

Imperiali *et al.* (*6*) were the first to develop a class of inhibitors that specifically target *OT in vitro*. The incorporation of γ-aminobutyrine (Amb) in the peptide *cyclo*(hex-Amb_1-Cys_2)-Thr_3-Val_4-Thr_5-Nph_6-NH_2 resulted in a potent inhibitor that exhibited slow, tight-binding inhibition of *OT* ($K_i = 37$ nM). Experimental evidence supports the bioactive conformer in the glycosylation consensus sequence (NXT/S) being an Asx-turn (for a recent review, see ref *7*), where the polypeptide backbone has a more extended conformation than a β-turn. The cyclized moiety of the inhibitor is constrained to an Asx-turn conformation, where the amine of Amb replaces the amide functionality of the Asn residue. A detailed examination of the *OT* exosites revealed that Val at position 4 and Thr at position 5 displayed the lowest K_i, consistent with the structure of the prototype inhibitor described above (*8*). This specific *OT* inhibitor was used as the prototype for designing new inhibitors to study the roles of glycosylation in cellular processes. Toward this goal, we have redesigned the prototype inhibitor using both passive and active membrane permeating strategies to target cellular *OT*.

The first approach employed in this study to make the prototype inhibitor membrane permeable incorporates an established membrane permeable tag. This peptide import function is based on a modified hydrophobic region of the signal sequence of Kaposi fibroblast growth factor (*9*). It has been used as the carrier for many cell permeable peptides (*10*) and has been shown to efficiently carry a number of peptides across the cell membrane, and even into the nucleus (*11*). The size of the cargo is seemingly irrelevant, as is exemplified by a 41 kDa glutathione *S*-transferase protein that was translocated into intact cells (*10*). The 12 amino acid residues of this membrane permeable sequence form an α-helix in solution and are believed to strongly interact with the lipids in the membrane, resulting in transport of the helix and cargo across a lipid barrier (*12*). Thus, this strategy explores a passive diffusion of the template inhibitor through the membrane bilayer of the ER (Figure 1a).

While the above inhibitor was redesigned to achieve transport by harnessing hydrophobic interactions with lipids in the ER membrane, an inhibitor with the ability to be shuttled through a specific channel in the lumen of the ER was also investigated. This active transport approach to translocating the inhibitor through the ER membrane targeted an ER surface receptor, the transporter associated with antigen processing (TAP) (Figure 1b). TAP translocates peptides from the cytosol into the lumen of the ER in an ATP-dependent manner. These peptides subsequently bind to and stabilize major histocompatibility complex (MHC) class I molecules (*13*). These peptide sequences are readily transported and can be glycosylated by *OT* on the lumenal side of the ER. This modification serves as a retention device in the lumen of the ER, allowing measurement of the translocated peptides (*14*), and can be utilized to assess the transport of the *OT* inhibitor TAP peptides across the ER. This ER transport system was chosen on the basis of the modest requirements for peptide acceptance by the TAP receptor. Species-specific selection is mainly restricted to the *C*-terminal residues, ideal for attachment to the prototype inhibitor cyclized at the amino-terminus. It has been shown that an 8−16 amino acid residue sequence is optimal for transport (*15*). Attachment of the small template inhibitor to the TAP recognition sequence easily accommodates this range. In addition, acylated *N*-termini and kinked (proline-containing) peptides have been shown to be transported into the ER (*16*), suggesting that the cyclized amino-terminus will retain ER transport ability.

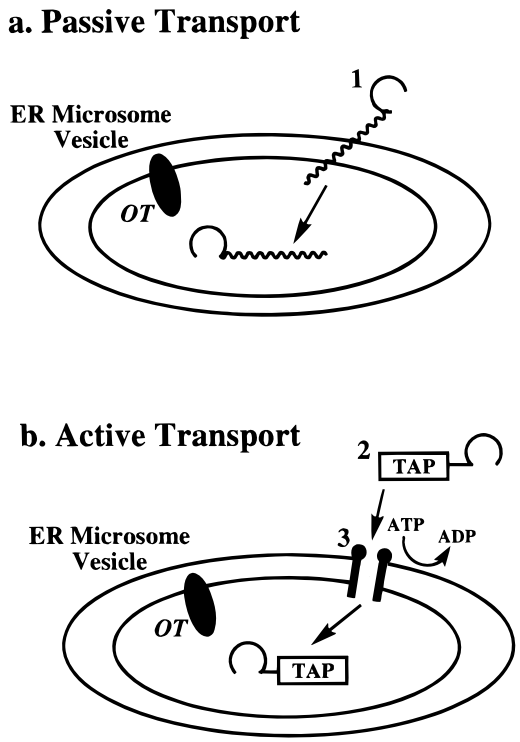

FIGURE 1: Cyclic inhibitor transport through an intact ER membrane for accessing *OT* in the lumen. (a) Passive transport of the redesigned inhibitor through the lipid bilayer, where **1** represents the cyclic inhibitor attached to a cell import function. (b) Active transport of the redesigned inhibitor *via* TAP machinery upon hydrolysis of ATP, where **2** represents the cyclic inhibitor attached to a TAP recognition peptide and **3** represents the TAP transporter.

We present herein an *in vitro* analysis of translocation through the ER membrane and glycosylation inhibition of the redesigned prototype inhibitor *via* both passive and active ER membrane diffusion approaches. An examination of cyclized glycosylation substrates provides evidence for translocation of the constrained moiety of the template inhibitor peptide. Finally, assessment of function in an ER model system is evaluated, completing the first study of *OT* inhibition in intact ER organelles.

MATERIALS AND METHODS

Peptide Synthesis. Amino acids and resins were purchased from PerSeptive Biosystems and Bachem, U.S.A. All other reagents were purchased from Sigma Chemical Co. and

Aldrich Chemical Co. Linear peptides and precursors were assembled by standard Fmoc (9-fluorenylmethoxycarbonyl) solid phase synthesis protocols (*17*) starting from Fmoc-PAL PEG resin (0.4 g, 0.17 mmol/g) or Fmoc-Pro-PEG-PS resin (0.5 g, 0.16 mmol/g) on a Milligen 9050 PepSynthesizer. Amino acids were coupled either as preactivated pentafluorophenyl esters or through the use of diisopropylcarbodiimide (DIPCDI) and 1-hydroxybenzotriazole (HOBt). Amino acids were used in the following side chain-protected forms: Amb(Boc), Asn(Tmob), Arg(Pbf), Cys(S-*t*Bu), Thr(*t*Bu), and Tyr(*t*Bu). Upon completion of the linear peptide synthesis, the amino-terminus was capped with a large excess of 6-bromohexanoic acid anhydride. The cysteine was deprotected under nitrogen in degassed dimethylformamide (DMF) using a large excess of tri-*n*-butyl phosphine (two 3 h treatments), followed by repeated washing of the resin with DMF. Cyclization was effected between the thiolate of cysteine and the 6-bromohexanoyl group in degassed DMF using a large excess of 1,1,3,3-tetramethylguanidine as a base (24 h) (*18*). Peptides were cleaved from the resin in a trifluoroacetic acid (TFA)/water/triisopropylsilane (TIPS) (95/5/5) mixture (3 h), triturated in diethyl ether (twice), redissolved in water/acetonitrile, and lyophilized to dryness.

All peptides were purified by preparative reverse phase high-pressure liquid chromatography (RP-HPLC) with a gradient elution (15−20% acetonitrile/water/0.1% TFA to 40−45% acetonitrile/water/0.1% TFA) over the course of 35 min, with a flow rate of 2.0 or 9.5 mL/min for semi-prep and prep C_{18} columns, respectively. Peptide identity was verified by electrospray mass spectrometry. The chromophore of the *p*-nitrophenylalanine or tyrosine allowed facile assessment of concentration (*19*). The concentration of those peptides without chromophores was measured by quantitative amino acid analysis.

Radioiodination of Peptides. Cyclized glycosylation substrates were labeled by chloramine-T-mediated iodination (*20*) to a specific activity of approximately 6 Ci/mmol. Morpholine (5 equiv based on peptide) was added to a solution of chloramine-T (20 equiv) in 50 μL of 0.1 M phosphate buffer (pH 7.5). After 1 min, $Na^{125}I$ (1 equiv) was added to the peptide solution [0.5 mM in 200 μL of 0.1 M phosphate buffer (pH 7.5)] in a separate Eppendorf tube from the morpholine reaction. After 1 min of the peptide reaction, the chloramine-T/morpholine solution was added to the peptide/^{125}I solution and allowed to react for 2 min. The reaction was quenched by the addition of $Na_2S_2O_3$ (30 equiv). Free iodine was removed by dialysis using a Spectrapor/CE Dispodialyzer (MWCO 500) from Spectrum (Laguna Hills, CA).

Oligosaccharyl Transferase Assays in Which Bz-Asn-Leu-Thr-NHMe (NLT) Substrate Was Used. A solubilized membrane of yeast (*Saccharomyces cerevisiae*) *OT* was prepared as described previously (*21*). Assays for the determination of inhibitor equilibrium dissociation constants (K_i) and substrate equilibrium constants (K_M) were performed as described previously (*8*).

Oligosaccharyl Transferase Assays in Which TAP Substrate Was Used. Assays were performed at room temperature in assay buffer [50 mM HEPES (pH 7.3), 150 mM KOAc, 5 mM MgOAc, 250 mM sucrose, and 1 mM dithiothreitol] in a total volume of 200 μL. The lipid-linked glycosyl donor dolichol-P-P-GlcNac-[^{3}H]GlcNAc ([^{3}H]-DPPC) was aliquoted into Eppendorf tubes (200 000 dpm at 60 Ci/mmol) from a chloroform/methanol stock solution. Aliquots were dried under a gentle stream of nitrogen. Increasing amounts of peptidyl inhibitor (in 10 μL of DMSO) and a constant amount of enzyme in buffer were incubated on ice for 30 min to pre-equilibrate the inhibitor with the enzyme. The reaction was initiated by the addition of 10 μL of 10 mM TAP substrate in H_2O. Aliquots (40 μL) were quenched into 200 μL of 4 mM $MnCl_2$ and 1 mL of chloroform/methanol (3/2) after 0.15, 2, 5, 8, and 15 min. The aqueous phase, containing radioactive N-glycosylated peptide, was extracted and quantified by the addition of 5 mL of EcoLite, and the counts per minute were measured in a Beckman LS 5000TD scintillation counter. K_i and K_M values were calculated as described previously (*8*).

Preparation of Mouse Microsomes for ^{125}I Assays. Microsomes were prepared essentially as described previously (*22*). Briefly, 10 female C57BL/6 mice 6−8 weeks of age were injected intraperitoneally with 0.2 mg of polyinosinic polycytidylic acid (Sigma) per mouse 24−36 h before being sacrificied *via* CO_2. Mice were injected, maintained, and sacrificed at the Beckman Behavioral Biology Animal Laboratory at the California Institute of Technology. The liver, spleen, and thymus were washed several times in homogenizing buffer [50 mM Tris-hydrochloride, 0.25 M sucrose, 2.5 mM $MgCl_2$, 3 mM dithiothreitol, and 0.1 mM AEBSF (pH 7.2)]. Homogenizing buffer was added (4 mL per gram of tissue), and the tissue was then homogenized in a Waring blender with glass beads, five passes up and down. The homogenate was centrifuged twice at 15000*g* for 15 min at 4 °C in a Beckman Ti 45 rotor. The supernatant was centrifuged (*23*) at 40000*g* for 2.5 h at 4 °C through a 1.3 M sucrose cushion in the homogenizing buffer (the load-to-cushion ratio was 3/1) in a Beckman model L7-55 ultracentrifuge. The rough microsome pellet was resuspended with a P1000 Gilson pipet in 1 mL of 50 mM HEPES, 250 mM sucrose, and 1 mM DTT (pH 7.3). Microsomes were snap frozen in liquid nitrogen in 50 μL aliquots and stored at −80 °C.

^{125}I Peptide Transport and Glycosylation Assays. Assays were assembled on ice as described previously (*24*). Each reaction mixture contained 60 nM [^{125}I]Thr-Tyr-Asn-Arg-Thr-Arg-Ala-Leu-Ile, 50 mM HEPES (pH 7.3), 150 mM KOAc, 5 mM MgOAc, 250 mM sucrose, 1 mM dithiothreitol, an ATP-generating system (50 mM ATP, 250 mM UTP, 2.5 mM creatine phosphate, 8 units of rabbit muscle creatine phosphokinase, and, where applicable, competitor peptides), and glycosylation machinery (1 μM Dolichol-P, 0.2 μM UDP-*N*-acetylglucosamine, 1 μM GDP-mannose, and 0.2 μM UDP-glucose) (*25*). Reaction mixtures were incubated for 10 min at room temperature. Microsomes were sedimented (15 min at 14000*g*) and the supernatants removed. Pellets were washed with 100 μL of assay buffer at 14000*g* for 10 min. Supernatants were pipetted off, and pellets were resuspended in 200 μL of lysis mix [0.5% NP-40, 150 mM Tris-hydrochloride (pH 7.4), 150 mM NaCl, and 5 mM $MgCl_2$] by repeated pipetting (Gilson 250 μL positive displacement pipet). Aliquots (20 μL) were added to 7 mL of EcoLite, and radioactivity was determined by γ-counting.

Cellular Assay and Metabolic Labeling with [^{35}S]Methionine. The cellular assay is based on a modified CHO

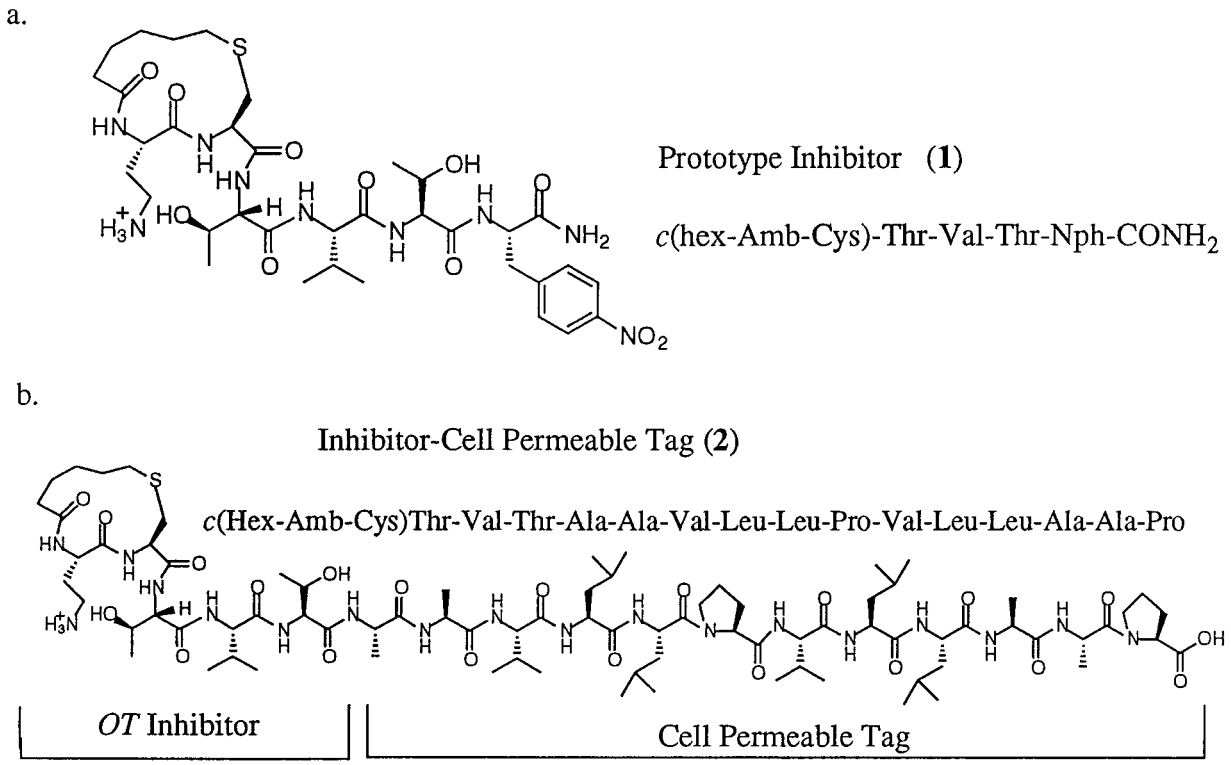

FIGURE 2: Structure and sequence of (a) the prototype *OT* inhibitor and (b) the redesigned inhibitor, including the prototype cyclized inhibitor moiety at the amino-terminus and a cell import function at the carboxy-terminus.

cell line, CHO 3.6, that secretes a m144 murine cytomegalovirus MHC class I homologue glycoprotein into media. Cells and the antibody were kindly donated by the Bjorkman Laboratory at the California Institute of Technology.

Day 1. Cells were harvested from monolayer culture flasks using 1 mmol of trypsin/EDTA and plated into 24-well cell culture plates at a density of 3×10^5 cells/well in 500 μL of α-MEM medium (containing 5% dialyzed fetal bovine serum, penicillin/streptomycin, and 100 μM L-methionine sulfoximine). The addition of inhibitors resulted in a final DMSO concentration of <2%. Cells were allowed to grow for approximately 24 h in 5% CO_2.

Day 2. The medium was aspirated, and cells were washed once with PBS. Modified Met-/Cys-DMEM (5% dialyzed fetal bovine serum, penicillin/streptomycin, and 100 μM L-methionine sulfoximine), 500 μL, was added along with the inhibitors and 5 μL of Trans ^{35}S label (metabolic labeling reagent ICN 51006) to each well. The plate was inserted into a tupperware container along with a dish of charcoal. One corner of the lid was left open to circulate the 5% CO_2 from the incubator to the cells. The plate was incubated for 5 h. The supernatants were removed and centrifuged to remove any cell debris. An antibody (6 ng) against m144 protein was added to each sample along with 50 μL of 1 M Tris-HCl (pH 7.5). Samples were rocked at 4 °C for 1 h. Suspended protein G beads, 30 μL (Pharmacia), were added to each sample, and rocking was continued for an additional 1 h at 4 °C. Beads were pelleted and washed three times with 1× PBS with 0.5% Triton X-100. After the final wash, beads were taken up in 15 μL of Laemmeli running buffer [2.2 mL of H_2O, 1 mL of 0.5 M Tris (pH 6.8), 0.8 mL of glycerol, 1.6 mL of 10% SDS, 0.4 mL of 0.8 M DTT, and 2 mL of 0.1% bromphenol blue]. Samples were boiled for 5 min, and the supernatant was loaded onto a 15% SDS−PAGE gel. Hyperfilm-MP (18 cm × 24 cm) was purchased from Amersham.

RESULTS

In Vitro Analysis of Glycosylation Inhibition by an OT Inhibitor−Cell Permeable Tag Peptide. The first approach to modifying the prototype inhibitor (Figure 2a, compound **1**) targeted a passive diffusion strategy. A membrane permeable *OT* inhibitor was created by addition of a cell import peptide onto the *C*-terminus of the root inhibitor (Figure 2b, the inhibitor−cell permeable tag is compound **2**). This hydrophobic tail was added to the cyclic inhibitor in an attempt to increase the lipophilicty of the molecule, enhancing its ability to permeate the ER membrane. The efficacy of **2** against *OT* was examined in competitive assays with the Bz-Asn-Leu-Thr-NHMe (NLT) substrate (*26*) using solubilized yeast microsomes. This type of microsome assay compares inhibitor potency without any assessment of ER membrane permeability. Previously, the prototype inhibitor (compound **1**), exhibiting a K_i of 37 nM (*6*), was found to be the most potent of any *OT* inhibitors characterized to date (*25*, *26*). Remarkably, kinetic analysis of the redesigned inhibitor (compound **2**) in this study revealed that this modified peptide exhibited a K_i of 41 nM, a value nearly identical to that of the root inhibitor (compound **1**). Regardless of the cell permeable extension to the root inhibitor, compound **2** displayed potent inhibition of *OT* in an *in vitro* ER assay.

Translocation across the ER Membrane. While detergent-solubilized microsomes are used to evaluate inhibitor potency, the employment of nonsolubilized microsomes allows the assessment of translocation into the lumen of the ER through an intact membrane, and therefore represents an ER

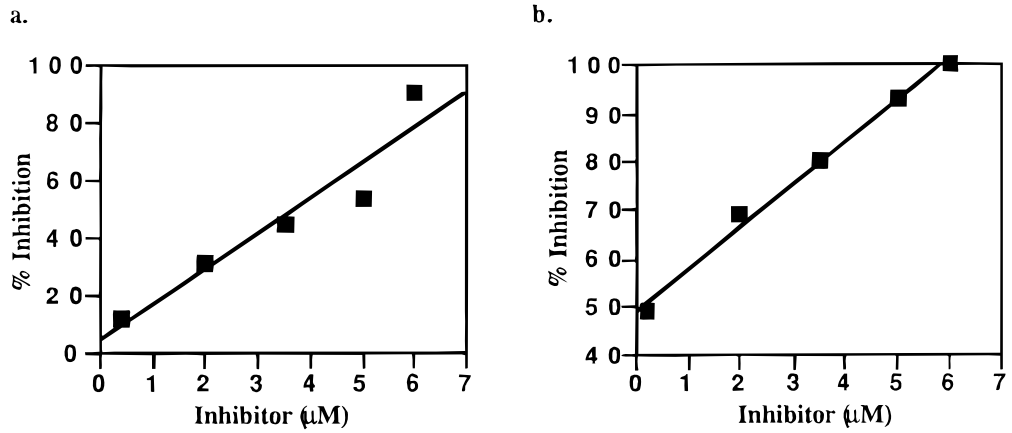

FIGURE 3: Increasing concentration of the inhibitor−cell permeable tag peptide gives linear OT inhibition of both a TAP and NLT glycosylation substrate in nonsolubilized microsomes. (a) Inhibition of a TAP substrate: 0.5 mM TAP glycosylation substrate with 0.4, 2.0, 3.5, 5.0, and 6.0 μM inhibitor. (b) Inhibition of an NLT substrate: 0.5 mM NLT glycosylation substrate with 0.2, 2.0, 3.5, 5.0, and 6.0 μM inhibitor.

Table 1: Parameters[a] from the *in Vivo* ER Assay for the Inhibitor−Cell Permeable Tag (Compound **2**)

substrate	IC_{50} (μM)	K_i (μM)
TAP (Tyr-Asn-Arg-Thr-Arg-Ala-Leu-Ile)	3.2 ± 1.1	2.6 ± 0.4
NLT	0.5 ± 2.9	0.05 ± 0.7

[a] The IC_{50} and K_i values from the inhibition of both a TAP and NLT glycosylation substrate were determined from the data displayed in Figure 3.

assay for potential inhibitors. Using intact ER organelles, the inhibitor−cell permeable tag peptide (compound **2**) displayed concentration-dependent inhibition of *OT*. This was shown by the decrease in the extent of glycosylation of two different substrates, TAP (Thr-Tyr-Asn-Arg-Thr-Arg-Ala-Leu-Ile) and NLT (Figure 3). The K_M for the latter substrate has been previously determined to be 240 μM (*26*). A K_M for TAP was measured in this assay to compare K_i values using both glycosylation substrates. Using a Hanes plot, the K_M for TAP in nonsolubilized microsomes was measured ($K_M = 170$ μM) and incorporated into the Segel equation (*27*) to afford a K_i for the inhibitor−cell permeable tag peptide using the TAP substrate. Inhibition constants for both substrates fell in the low micromolar range for this ER assay (Table 1). The IC_{50} values listed in Table 1 are useful in comparing the potencies of inhibitors using the same substrate. However, the K_i values take into account the substate equilibrium constant, K_M, and are therefore normalized values with which to compare inhibitor potencies with various substrates. Given the heterogeneity of microsomal preparations, the parameters varied between assays, and hence, all data were accumulated from the same stock of prepared vesicles. The inhibition of glycosylation demonstrated by **2** suggests that the compound accomplishes translocation through the ER membrane while retaining potent inhibition of *OT*. However, to achieve inhibition in intact cells, the outer cell membrane must also be crossed. Preliminary results from a whole cell assay indicated that inhibition of glycosylation did not occur upon addition of this redesigned inhibitor (up to 100 μM compound **2**, data not shown).

Design and Synthesis of OT−Inhibitor−TAP Peptides. The second approach to redesigning the prototype inhibitor employed a nine amino acid peptide (Thr-Tyr-Gln-Arg-Thr-Arg-Ala-Leu-Ile) previously found to be ideal for mouse TAP translocators (*14*). The cyclized prototype inhibitor was appended to the last eight residues of this sequence (the Thr was deleted due to the occurrence of this amino acid in the prototype inhibitor). A family of redesigned inhibitor−TAP peptides was assembled, including both cyclized (Figure 4, compounds **3** and **4**) and linear inhibitor sequences (Figure 4, compounds **5** and **6**), to compare the efficiencies of translocation into the ER. The first synthesized cyclic inhibitor−TAP peptide (compound **3**) included Val and Thr residues at positions 4 and 5, respectively, to increase the *OT* binding affinity (*8*). A cyclized inhibitor−TAP peptide was synthesized without the Val and Thr residues to study translocation efficiency with a shorter peptide (compound **4**). Given the optimal nine amino acid residues of the root TAP peptide, the shortened inhibitor conforms more to this length, resulting in a sequence of 12 residues. Derivatives containing both a Thr residue (compound **5**) and a Ser residue (compound **6**) at the amino-terminus of the linear inhibitor−TAP peptides were synthesized. Previous studies have found the Thr residue to be more ideal for TAP, while the Ser residue is optimal for *OT* binding (*28*).

In Vitro Analysis of Glycosylation Inhibition by OT Inhibitor−TAP Peptides. Kinetic analysis of the inhibitor−TAP peptides in detergent-solubilized microsomes (Table 2) revealed that the extended cyclized inhibitor−TAP peptide (compound **3**) also retained nanomolar inhibition potency ($K_i = 97$ nM), similar to that of compound **2** and the root inhibitor peptide (compound **1**) ($K_i = 37$ nM; *6*). The cyclic inhibitor−TAP peptide without the additional Val and Thr exosite residues (compound **4**) demonstrated a modest K_i (1.4 μM). As expected, the linear inhibitors (compounds **5** and **6**) competed weakly ($K_i = 120-130$ μM for both). Although these peptides are much less potent inhibitors than their cyclized counterparts, the TAP machinery may shuttle the linear peptides more efficiently. These results reinforce the TAP strategy for redesigning the cyclized peptides which includes TAP features without interfering with the inhibitory potency.

Transport and Glycosylation of Cyclized TAP Substrates. Before examination of TAP translocation of the redesigned inhibitors, any indirect inhibition occurring from the cyclized moiety of the inhibitor−TAP peptides was assayed. For

a. Inhibitor-TAP (**3**)

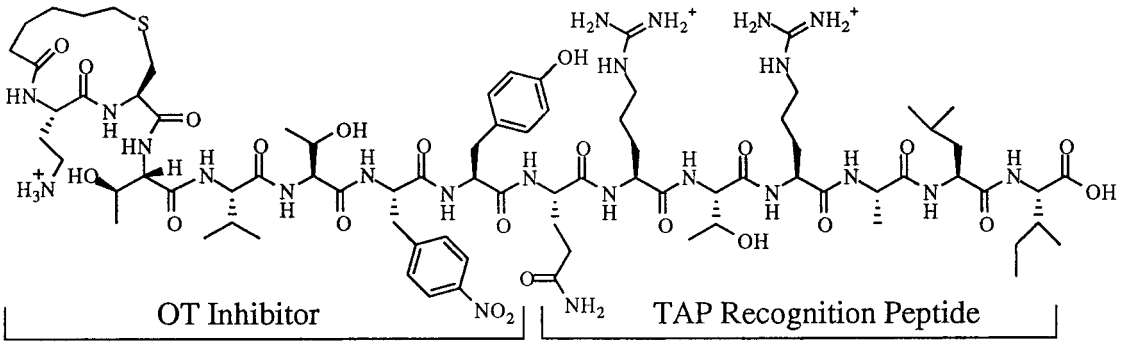

c(hex-Amb-Cys)-Thr-Val-Thr-Nph-Tyr-Gln-Arg-Thr-Arg-Ala-Leu-Ile

Cyclized Inhibitor-TAP Peptides
- *c*(hex-Amb-Cys)-Thr-**Val-Thr**-Nph-TAP Sequence (**3**)
- *c*(hex-Amb-Cys)-Thr-Nph-TAP Sequence (**4**)

Linear Inhibitor-TAP Peptides
- NH_2-**Thr**-(Amb-Leu-Thr)-Val-Thr-Nph-TAP Sequence (**5**)
- NH_2-**Ser**-(Amb-Leu-Thr)-Val-Thr-Nph-TAP Sequence (**6**)

b. TAP Sequence = Tyr-Gln-Arg-Thr-Arg-Ala-Leu-Ile

FIGURE 4: (a) Structure and sequence of the *OT* inhibitor−TAP peptide incorporating the prototype cyclized inhibitor moiety at the amino-terminus and the TAP features at the carboxy-terminus and (b) a family of inhibitor−TAP peptides, including both cyclized and linear sequences.

Table 2: *In Vitro* Analysis of Glycosylation Inhibition by *OT* Inhibitor−TAP Peptides in Solubilized Microsomes[a]

inhibitor−TAP peptide	K_i (μM)	inhibitor−TAP peptide	K_i (μM)
1	0.37	**5**	120−130
3	0.97	**6**	120−130
4	1.4		

[a] Refer to Figures 2a and 4a for the peptide numbering scheme.

example, once bound to TAP on the surface of the ER, the bulky cyclic constituent could block translocation of the glycosylation substrates by TAP, resulting in a false measurement of *OT* inhibition. Translocation and subsequent glycosylation of cyclized TAP substrates would provide evidence for the acceptance of the cyclized inhibitors to be transported by the TAP receptor. The cyclized substrates are identical in sequence to inhibitor−TAP peptides **3** and **4**, except an Asn replaces the Amb, resulting in the Asn-Cys-Thr glycosylation consensus sequence embedded in the cyclic component of the peptides. Both substrates exhibited K_Ms in the low micromolar range in the above *in vitro* kinetic assays using solubilized microsomes (0.130 and 0.223 μM for substrates analogous to **3** and **4**, respectively), indicative of efficient substrates for *N*-linked glycosylation.

To quantitatively determine the efficiency of the translocation of cyclized TAP glycosylation substrates across the ER membrane *via* TAP machinery, peptide substrates were radioiodinated and assayed in mouse microsomes. Figure 5 shows that the cyclized TAP substrates were translocated and glycosylated approximately 30−50% as efficiently as the TAP substrate. Due to the acceptance of the cyclized TAP substrates into the microsomes through the TAP translocators on the surface of the membrane, inhibition of glycosylation by the cyclized inhibitor−TAP peptides can be attributed to specifically targeting *OT* inhibition after translocation.

Study of the Translocation of the Cyclized Inhibitor−TAP Peptides by TAP Machinery. The addition of the extended cyclized inhibitor−TAP peptide (compound **3**), the most potent of the redesigned TAP family of inhibitors, to the above radioiodinated assay did not result in any observed inhibition in intact ER membranes up to 100 μM inhibitor peptide (data not shown). The linear inhibitors, having much

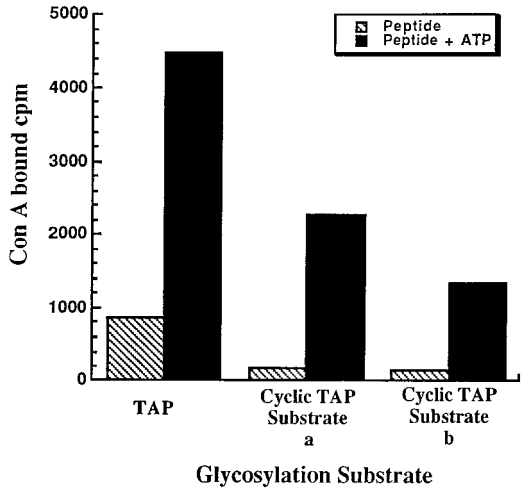

FIGURE 5: TAP substrate glycosylation in mouse microsomes. TAP is Thr-Tyr-Asn-Arg-Thr-Arg-Ala-Leu-Ile: (a) cyclic TAP substrate *cyclo*(hex-Asn-Cys)-Thr-Val-Thr-Nph-TAP sequence and (b) cyclic TAP substrate *cyclo*(hex-Asn-Cys)-Thr-Nph-TAP sequence. All peptides were radioiodinated with ^{125}I, and the counts per minute were counted on the basis of the ^{125}I-glycosylated peptide bound to concavalin A. Without the addition of ATP, the extent of glycosylation of all three peptides was negligible.

higher K_is, were not assayed. To confirm that the inhibitors were not transported by TAP, compounds **3** and **4** were evaluated with solubilized microsomes using the TAP substrate rather than the NLT substrate that was used previously. The inhibitors successfully prevented glycosylation of this substrate displaying a K_i of 3.8 μM, confirming that the lack of TAP translocation of the cyclized inhibitor peptides was the reason for the failed inhibition in an intact ER membrane.

DISCUSSION

The cyclic peptide *cyclo*(hex-Amb-Cys)-Thr-Val-Thr-Nph-NH_2 (compound **1**) had been previously shown to be the most potent inhibitor of *OT* in *in vitro* kinetic analyses (*6*, *8*). To gain an improved understanding of the cellular role of *OT* in the *N*-linked glycosylation process, the prototype inhibitor was redesigned to permeate the ER membrane utilizing both passive and active transport strategies. First, the inhibitor template was modified to include a membrane permeable tag (compound **2**) in an attempt to accomplish passive transport into the lumen of the ER. This redesigned inhibitor was successfully translocated into the lumen of an intact ER membrane and displayed subsequent potent inhibition of *OT*. Although this compound did not exhibit inhibition in a whole cell study, given the characteristics of this assay, the conclusions that can be drawn from these findings are limited. For example, although the results indicated that inhibition of glycosylation did not occur, this assay provides no information about the inhibitor localization. In addition, since this carrier sequence has been previously shown to carry peptides through the cell membrane efficiently (*10*), the inhibitor may have been inactivated by proteolysis upon reaching the cytoplasm. This is currently under investigation.

In addition to seeking ER transport through passive diffusion, we modified the root inhibitor to include features recognized by the TAP machinery. This resulted in retention of nanomolar inhibition in kinetic analysis with the extended cyclized inhibitor−TAP peptide (compound **3**), regardless of the carboxy-terminal extension. These results, in combination with the nanomolar inhibition displayed by compound **2**, are indicative of a template inhibitor potent enough to withstand significant alterations in the overall size of the peptide. This readily modifiable prototype has prompted an exploration in modifying the *OT* exosites of this peptide to enhance the permeability of the root peptide without extensions.

After demonstrating potent inhibition of the redesigned inhibitors in *in vitro* kinetic analyses, we evaluated the transport of the inhibitor−TAP peptides by TAP machinery. Efficient translocation and glycosylation of the cyclized TAP substrates were demonstrated in intact microsomes. These studies indicated that the cyclized moiety was successfully transported to the lumen of the ER. Presumably, therefore, the cyclized portion of the inhibitor−TAP peptides would not hinder substrate translocation through TAP channels, effecting indirect inhibition of *OT*. When the redesigned TAP inhibitors (compounds **3** and **4**) were used in this study, no inhibition of *OT* was measured. Although the cyclized inhibitor−TAP peptide structure is very similar to that of the cyclized substrate, they differ in overall charge. Since the neutrally charged cyclized TAP substrates were not only translocated by TAP, but also efficiently glycosylated, the lack of TAP transport of the inhibitor was attributed to the charged amine functionality at the amino-terminus of the cyclized moiety. Future inhibitor designs can therefore be adapted to modify this feature of the compounds.

The two strategies evaluated in this study were passive diffusion through an interaction with the lipids in the ER membrane and active transport through the TAP channel. The inhibitor−cell permeable tag (compound **2**) achieved passive translocation across an intact ER membrane and subsequent potent inhibition of *OT*. This study represents the first step toward studying inhibition of *OT in vivo* by successfully transporting a modified inhibitor across the intracellular ER membrane. Future studies can now focus on further refining the structure of the prototype inhibitor in a systematic manner to provide *OT* inhibitors that function in the cellular environment.

REFERENCES

1. Kaplan, H. A., Welply, J. K., and Lennarz, W. J. (1987) *Biochim. Biophys. Acta 906*, 161−173.
2. Marshall, R. D. (1972) *Annu. Rev. Biochem. 41*, 673−702.
3. Keller, R. K., Boon, D. Y., and Crum, F. C. (1979) *Biochemistry 18*, 3946−3952.
4. Duksin, D., and Mahoney, W. C. (1982) *J. Biol. Chem. 257*, 3105−3109.
5. Tamura, G. (1982) *Tunicamycin*, Japan Scientific Society Press, Tokyo.
6. Hendrickson, T. L., Spencer, J. R., Kato, M., and Imperiali, B. (1996) *J. Am. Chem. Soc. 118*, 7636−7637.
7. Imperiali, B., and O'Connor, S. E. (1998) *Pure Appl. Chem. 70* (1), 33−40.
8. Kellenberger, C., Hendrickson, T. L., and Imperiali, B. (1997) *Biochemistry 36*, 12554−12559.
9. Delli Bovi, P., Curatola, A. M., Kern, F. G., Greco, A., Ittmann, M., and Basilico, C. (1987) *Cell 50*, 729−737.
10. Rojas, M., Donahue, J. P., Tan, Z., and Lin, Y.-Z. (1998) *Nat. Biotechnol. 16*, 370−375.
11. Lin, Y.-Z., Yao, S., and Hawiger, J. (1996) *J. Biol. Chem. 271*, 5305−5308.

12. Du, C., Yao, S., Rojas, M., and Lin, Y.-Z. (1998) *J. Pept. Res. 51*, 235−243.
13. Heemels, M.-T., and Ploegh, H. (1995) *Annu. Rev. Biochem. 64*, 463−491.
14. Heemels, M.-T., Schumacher, T. N. M., Wonigeit, K., and Ploegh, H. L. (1993) *Science 262*, 2059−2063.
15. Momburg, F., Roelse, J., Hammerling, G. J., and Neffjes, J. J. (1994) *J. Exp. Med. 179*, 1613−1623.
16. Neefjes, J., Gottfried, E., Roelse, J., Gromme, M., Obst, R., Hammerling, G., and Momburg, F. (1995) *Eur. J. Immunol. 25*, 1133−1136.
17. Atherton, E., and Sheppard, R. C. (1989) *Solid phase peptide synthesis*, Oxford University Press, New York.
18. Virgilio, A. A., and Ellman, J. A. (1994) *J. Am. Chem. Soc. 116*, 11580−11581.
19. Pace, C. N., Vajdos, F., Fee, L., Grimsley, G., and Gray, T. (1995) *Protein Sci. 4*, 2411−2423.
20. Hunter, W. M., and Greenwood, F. C. (1962) *Nature 194*, 495−496.
21. Pathak, R., Hendrickson, T. L., and Imperiali, B. (1995) *Biochemistry 34*, 4179−4185.
22. Shepherd, J. C., Schumacher, T. N. M., Ashton-Richardt, P. G., Imaeda, S., Ploegh, H. L., Janeway, C. A., Jr., and Tonewaga, S. (1993) *Cell 74*, 577−584.
23. Walter, P., and Blobel, G. (1983) *Methods Enzymol. 96*, 84−93.
24. Schumacher, T. N. M., Kantesaria, D. V., Heemels, M.-T., Ashton-Rickardt, P. G., Shepherd, J. C., Fruh, K., Yang, Y., Peterson, P. A., Tonegawa, S., and Ploegh, H. L. (1994) *J. Exp. Med. 179*, 533−540.
25. Rathod, P. K., Tashjian, A. H., Jr., and Abeles, R. H. (1986) *J. Biol. Chem. 261*, 6461−6469.
26. Imperiali, B., Shannon, K. L., Unno, M., and Rickert, K. W. (1992) *J. Am. Chem. Soc. 114*, 7944−7945.
27. Segel, I. H. (1975) *Enzyme Kinetics*, Wiley, New York.
28. Gavel, Y., and von Heijne, G. (1990) *Protein Eng. 3* (5), 433−442.

BI982740E